JOURNAL OF RENEWABLE ENERGY AND SMART GRID TECHNOLOGY

Vol. 20, No. 1, January-June 2025

Artificial Neural Network Estimation of Daily Net Radiation Using Meteorological Data in Thailand

Chutimon Phoemwong, Rungrat Wattan*, Serm Janjai

Department of Physics, Faculty of Science, Silpakorn University, Muang, Nakhon Pathom 73000, Thailand

***Corresponding author's email**: rungrat.wattan@gmail.com

Article info:

Received: 17 October 2024
Revised: 3 December 2024
Accepted: 15 January 2025
DOI:
10.69650/rast.2025.259017

Keywords:

Net Radiation
Artificial Neural Network
Meteorological Data

ABSTRACT

Net radiation is the difference between downward and upward radiation, considering both shortwave and longwave radiation. The net radiation controls the water cycle, plant photosynthesis, the earth's climate changes, and the energy balance. In this paper, the Artificial Neural Network (ANN) model is developed for estimating daily net radiation from meteorological data that are based on maximum air temperature, minimum air temperature, daily relative humidity, and daily solar radiation. Net radiation and meteorological data collected for 7 years (2017-2023) from Chiang Mai meteorological station (CM: 18.77°N, 98.96°E), Ubon Ratchathani meteorological station (UB: 15.24°N, 105.02°E), Nakhon Pathom meteorological station (NP: 14.01°N, 99.96°E), and Songkhla meteorological station (SK: 7.41°N, 100.62°E) were used to train and test the model. The discrepancy between the net radiation estimated by the ANN and the measured net radiation was presented in terms of determination coefficient (R^2), relative root mean square error (RMSE), and relative mean bias error (MBE). The model showed 0.98, 14.48%, and -2.17%, respectively. The result shows that the artificial neural network model is an accurate and easy option for estimating surface net radiation.

1. Introduction

Net radiation is the sum of net shortwave and net longwave radiation. The source of shortwave radiation is the sun, its spectral wavelength range of 0.25 to 4.00 micrometers. It includes ultraviolet radiation, visible light, and infrared radiation. Longwave radiation is thermal radiation emitted by the Earth's surface and the atmosphere, its spectral wavelength range between 3.00 and 100.00 micrometers. The difference between downward shortwave and upward shortwave radiation is net shortwave radiation, while the difference between downward and upward longwave radiation is net longwave radiation. So, the net radiation can be calculated with equations (1-2).

$$R_n=(DS-US)+(DL-UL) \quad (1)$$

$$R_n=DS(1-\alpha)+(DL-UL) \quad (2)$$

Where DS and US are the surface downward and upward shortwave radiation (MJ/m^2), DL and UL are the surface downward and upward longwave radiation (MJ/m^2), α is surface albedo (dimensionless), and R_n is surface net radiation (MJ/m^2).

Net radiation regulates various phenomena on Earth, especially energy balance and climate change. The positive value of R_n indicates that more incoming radiation than outgoing radiation leads to warming of the Earth's surface and the atmosphere. The negative value of R_n indicates that more outgoing radiation than incoming radiation, leads to cooling of the Earth's surface and the atmosphere. And the zero net radiation indicates that incoming and outgoing radiation is balanced, resulting in no net radiation change in temperature. The sample of global warming research, such as in 2021, Ojo et al. studied the effect of the radiation balance on the warming event, was evaluated using a cross-correlation technique. The result shows a decrease in net radiation because of dominant upward longwave radiation components that determine the warming effect on the surface of the earth [1]. Besides, increases or decreases in net radiation affect the dissolution of ice in polar areas. In the case of hydrological research assessed, the accuracy of estimating evapotranspiration (ET_0) using the FAO-56 Penman-Monteith (FAO-56-PM) model, with measured and estimated net radiation. The results indicate that changes in evaporation are primarily driven by changes in net radiation at the surface [2-3] therefore, net radiation is crucial. The limited installation of net radiation measurement instruments, especially in Thailand, there is a significant gap in the data required for accurate evapotranspiration estimation.

Net radiation can be measured using a net radiometer, which consists of two pyranometers for measuring downward and upward shortwave radiation (DS and US) and two pyrgeometers for measuring downward and upward longwave radiation (DL and UL). However, it is expensive, requires annual calibration, and is time-consuming. Therefore, researchers have developed models to estimate net radiation in areas where measurement instruments are not installed. Many theoretical and empirical relations have been developed over the years. In 2009, Wang and Liang introduced a

model designed to estimate surface daytime net radiation. This model relied on a combination of solar radiation measurements and conventional meteorological data, such as daily minimum temperature, daily temperature range, and relative humidity, as essential inputs for its calculations [4]. In 2003, Irmak et al. [5] developed two alternative equations to reduce the input and computation intensity of the FAO56-Rn procedures to predict daily Rn and evaluate the performance of these equations in the humid regions of the southeast and two arid regions in the United States. The equation requires daily maximum air temperature (T_{max}), daily minimum air temperature (T_{min}), mean daily relative humidity (RH_{mean}), and solar radiation (R_s), which can be shown in equation (3). The model results showed a high performance of agreement with the ground-based measurements.

$$R_n = -0.09T_{max} + 0.203T_{max} - 0.101RH_{mean} + 0.687R_s + 3.97 \quad (3)$$

Where R_s is daily solar radiation (MJ/m^2), T_{max} is daily maximum air temperature (°C), T_{min} is daily minimum air temperature (°C), and RH_{mean} is mean daily relative humidity (%).

In 2003, Alados et al. studied net radiation in a semi-arid area in southeastern Spain, considering the relationship between net radiation and solar radiation at 5-minute intervals over 38 months. The model using solar radiation as an input variable can adequately estimate net radiation, and the relationship can be expressed by equation (4). Similar studies conducted in Thailand will be discussed in the following section [6].

$$R_n = 0.565R_s - 14.75 \quad (4)$$

Where R_s is solar radiation (W/m^2). In addition to meteorological parameters, Carmona et al. (2015) developed a method to estimate net radiation from remote sensing data obtained from Landsat 5 and 8 [7].

In the part of Thailand, Limhoon and Bualert [8] studied in Phetchaburi Province, Thailand, revealed that net radiation peaked during the summer, rainy and winter seasons, respectively. Furthermore, Tohsing et al. [9] developed the model for estimating net radiation from solar radiation in Thailand's main regions, namely Chiang Mai, Ubon Ratchathani, Nakhon Pathom, and Songkhla, from 2017 to 2021. The results, expressed in terms root mean square difference and mean bias difference, show good correspondence between the model data and the measured data and the relations can be expressed by equation (5).

$$\begin{aligned} R_n &= 0.600R_s - 0.407 \quad \text{(CM)} \\ R_n &= 0.503R_s + 0.957 \quad \text{(UB)} \\ R_n &= 0.620R_s - 0.594 \quad \text{(NP)} \\ R_n &= 0.595R_s - 0.090 \quad \text{(SK)} \end{aligned} \quad (5)$$

Where R_s is solar radiation (MJ/m^2).

However, due to the widespread study of artificial neural networks and machine learning in the present day. In 2011, Antonio Ferreira et al. evaluated the performance of artificial neural network (ANN) models in estimating net radiation (R_n) at the surface, compared to traditional linear models (LM). The ANN models were trained on meteorological data such as wind speed, wind direction, surface and air temperature, relative humidity, and soil moisture. The LM models required additional input in the form of solar incoming shortwave radiation measurements. Both ANN and LM models were tested against in-situ measurements. While the LM models achieved respectable results, the ANN models outperformed them in some cases. This suggests that ANN models can provide accurate estimates of net radiation without relying on solar radiation measurements [10]. In 2014, Jiang et al. studied the performance of two artificial neural network (ANN) models, general regression neural Networks (GRNN) and Neuroet package (It is an implementation of a multi-layer perceptron neural network, this package not only trains ANN models and makes predictions but also reverse-engineers them to extract underlying equations, revealing the significance of input variables.), in estimating global net all-wave surface radiation (R_n). These models were trained on a combination of remote sensing data, surface measurements, and meteorological reanalysis products. The ANN models were tested against in-situ measurements from 251 global sites between 1991 and 2010**.** Results showed that both ANN models outperformed traditional linear models, with GRNN demonstrating superior performance and stability compare to Neuroet [11]. So, in this research, the variation of net radiation and estimate net radiation from meteorological data and solar radiation being during the years 2017-2023 using the multi-layer feed-forward ANN model were studied at the main stations in Thailand. The ANN model can recognize and learn intricate patterns within large and complex datasets, it is highly adaptable and can learn from experience, and robust to noise and missing data.

2. Materials and methods

2.1 The instruments and net radiation data

The net radiation can be measured by a net radiometer, which has many models. It consists of two pyranometers for measuring downward and upward shortwave radiation, two pyrgeometers for measuring downward and upward longwave radiation, and one PT-100 temperature sensor for measuring the instrument's temperature. In this research, the CNR4 net radiometer of Kipp&Zonen are used, which is installed in a meteorological field at an altitude between 1.5 and 2 meters from the surface. It is shown in Fig. 1.

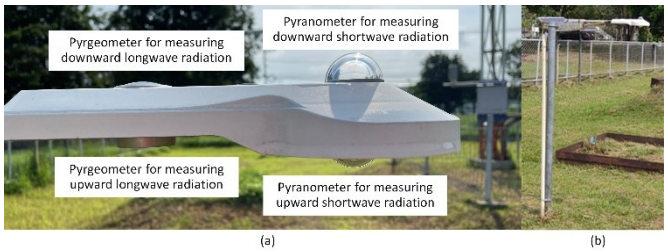

Fig. 1 (a) the component of the CNR4 net radiometer (Kipp&Zonen) and (b) the altitude of instruments between 1.5 and 2 meters.

Four meteorological stations equipped with net radiometers have been strategically installed across Thailand to capture the diverse climatic and geographical conditions of the country. Chiang Mai meteorological station (CM): Located at 18.77°N, 98.96°E in northern Thailand, this station is nestled amidst a mountainous landscape characterized by steep slopes, deep valleys, and lush forests. The region experiences a tropical climate, albeit cooler and less humid compared to other parts of the country. Ubon Ratchathani meteorological station (UB): Situated at 15.24°N, 105.02°E in northeastern Thailand, this station is positioned on a vast plain, a dominant feature of the region. The tropical climate here is characterized by distinct wet and dry seasons. Nakhon Pathom meteorological station (NP): Located at 14.01°N, 99.96°E in central Thailand, this station is situated on a fertile plain. The region's tropical savanna climate is marked by well-defined wet

and dry seasons. Songkhla meteorological station (SK): Located at 7.41°N, 100.62°E in southern Thailand, this station is situated in a diverse region characterized by coastal plains, lagoons, and hilly areas. The tropical monsoon climate of this region is influenced by the proximity to the sea. By strategically placing these stations, we can gain valuable insights into the variations in net radiation across Thailand's diverse geographical and climatic regions. The field meteorological had instruments installed, as shown in Fig. 2.

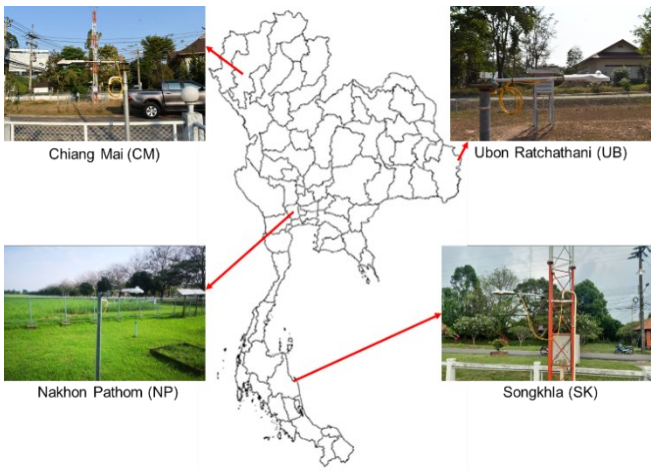

Fig. 2 The net radiometer of four stations in Thailand.

From the instrument, a voltage signal from four radiation sensors and a temperature signal from a temperature sensor were obtained. Data was recorded every second using a datalogger (Yokogawa, model FX-1012) and subsequently converted into radiation intensity measured in watts per square meter. This allowed us to calculate the values of radiation equations (6-9).

$$DS = \frac{V_{DS}}{C_{DS}} \tag{6}$$

$$US = \frac{V_{US}}{C_{US}} \tag{7}$$

$$DL = \frac{V_{DL}}{C_{DL}} + \sigma T^4 \tag{8}$$

$$UL = \frac{V_{UL}}{C_{UL}} + \sigma T^4 \tag{9}$$

Where DS, US, DL, and UL are downward shortwave radiation, upward shortwave radiation, downward longwave radiation, and upward longwave radiation, respectively. V_{DS}, V_{US}, V_{DL} and V_{UL} are voltage signals from DS, US, DL and UL sensors, respectively. C_{DS}, C_{US}, C_{DL} and C_{US} are sensitivity of DS, US, DL, and UL sensors, respectively, which is obtained from annual calibration. σ are Stefan Boltzmann's constant $\left(5.67 \times 10^{-8}\ W \cdot m^{-2} \cdot K\right)$, and T is temperature from temperature sensor in Kelvin. Then calculate net radiation in watts per square meter using equation (1). Filter the measurement data by getting rid of incorrect or impossible data, including data of instrument failure time. The statistical study of net radiation during 2017-2023 is shown in Table 1 and Fig. 3.

Table 1 The values of monthly average daily net radiation data.

Stations	Values			
	Max	Min	Mean	STD
CM	18.09	-0.16	9.98	3.08
UB	18.74	1.42	11.42	2.71
NP	18.47	0.56	10.99	2.91
SK	19.14	0.03	11.18	3.36

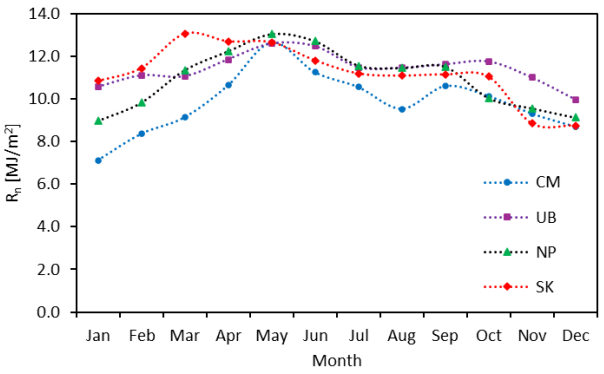

Fig. 3 The graph shows the long-term monthly average net radiation values of four stations in Thailand.

From Fig. 3, the monthly variation of net radiation in Thailand peaks in May, as this period experiences relatively high solar radiation and surface moisture due to the onset of the rainy season, this results in lower surface reflectivity. Effected by an increase in downward radiation and a decrease in upward radiation, ultimately resulting in high net radiation values. Except for SK Station, which has a different breeding season than other areas, the SK Station has net radiation values peak in March. After that the net radiation decreases and then returns to higher values again during the summer.

2.2 Meteorological data

A recent study by Aweda and Adebayo (2020) estimated net radiation using meteorological data obtained from a USB wireless weather station. A wide range of meteorological data was analyzed using simple empirical methods, yielding satisfactory results [12]. Nowadays, machine learning is widely used in data analysis, such as the artificial neural network model for estimating the soil temperature at 5, 10, 20, 50, and 100 cm depths using standard geographical and meteorological data considering altitude, latitude, longitude, month, year, monthly solar radiation, monthly sunshine duration, and monthly mean air temperature. The resulting model showed good agreement between the ANN-estimated soil temperature and the measured soil temperature [13]. And Patel et al. (2022) reviewed various algorithms, including those based on artificial neural networks (ANNs), such as feed-forward back-propagation ANN, multi-layer feed-forward ANN, linear regression with ANN, and Graph Neural Network (GNN), for estimating solar radiation and solar energy [14]. So, in this research, daily net radiation from meteorological data in the main region of Thailand using an artificial neural network model was estimated. We chose the locations of the stations as follows: Chiang Mai meteorological station, Ubon Ratchathani meteorological station, Nakhon Pathom meteorological station, and Songkhla meteorological station.

The meteorological data collected consists of daily maximum air temperature, daily minimum air temperature, daily mean relative humidity, and daily solar radiation because these parameters have a positive or negative correlation with net radiation and can be measured at every station. We control the quality of meteorological data by removing erroneous and impossible data. The statistical values of meteorological data are shown in Table 2.

Table 2 The statistical values of monthly average daily meteorological data.

Stations	Meteorological parameters	Values			
		Max	Min	Mean	STD
CM	Maximum temperature (°C)	42.20	20.00	33.77	2.91
	Minimum temperature (°C)	29.00	10.50	23.02	3.07
	Solar radiation (MJ/m^2)	27.89	1.79	17.77	4.45
	Relative humidity (%)	94.00	36.00	69.97	10.65
UB	Maximum temperature (°C)	40.90	17.80	33.62	2.84
	Minimum temperature (°C)	28.70	9.50	22.68	3.08
	Solar radiation (MJ/m^2)	27.81	2.27	18.91	4.36
	Relative humidity (%)	97.00	53.00	75.97	9.06
NP	Maximum temperature (°C)	41.10	20.60	33.73	2.74
	Minimum temperature (°C)	29.20	11.70	23.70	2.65
	Solar radiation (MJ/m^2)	27.65	1.29	18.25	4.62
	Relative humidity (%)	99.00	53.00	78.90	7.02
SK	Maximum temperature (°C)	41.10	24.50	32.64	2.29
	Minimum temperature (°C)	28.40	21.90	25.39	1.01
	Solar radiation (MJ/m^2)	28.32	0.45	19.09	5.54
	Relative humidity (%)	95.00	64.00	78.88	5.25

2.3 Methodology

From the data, we obtained meteorological data and net radiation data for input and validated the model, which is an artificial neural network model.

Artificial neural networks are mathematical models that learn and create nonlinear relationships between two datasets, which can discover intricate patterns [15,16]. It mimics the functioning of neuron cells, which receive data from the input layer, process data by active function in a node, and send the data to the output layer. The structure of a node is shown in Fig. 4, where w_1, w_2, …, and w_k are the weights at the inputs, and β is bias of the layer. Initialize the weights and biases, random values are typically assigned. Then, during the forward propagation phase, input data to the input layer moving to the hidden layers and finally to the output layer. At each neuron (node), the output is computed using the formula of summation and passed through an activation function. Then, calculate the loss by comparing the predicted output with the actual target values using a loss function, such as Mean Squared Error. This loss informs the back-propagation process, where gradients of the loss with respect to the weights and biases are computed, and the weights and biases are updated using gradient descent to minimize the loss [17-18]. These steps are repeated for multiple epochs until satisfactory performance is achieved. These nodes are arranged in a series of layers that together constitute the artificial neural network, the structure of the ANN model in this research, as shown in Fig. 5. The operation flowchart can be represented as shown in Fig. 6. The ANN model must have data for training, which accounts for 70% of all data. In this work, we use data from 2017-2021, and the remaining 30% is used for testing the model from 2022-2023. Except for the Songkhla meteorological station, which uses data from 2018-2022 as training data and data from 2023 as test data, due to the presence of anomalies in the input data during the 2017 period.

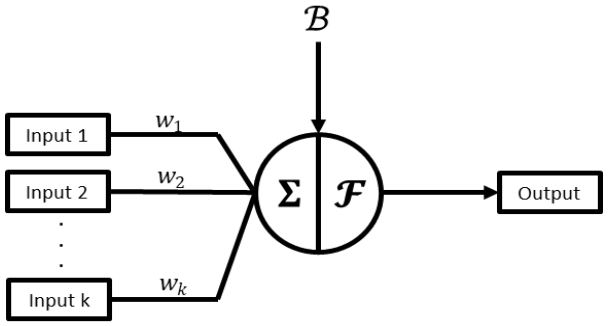

Fig. 4 The structure of a node in ANN model.

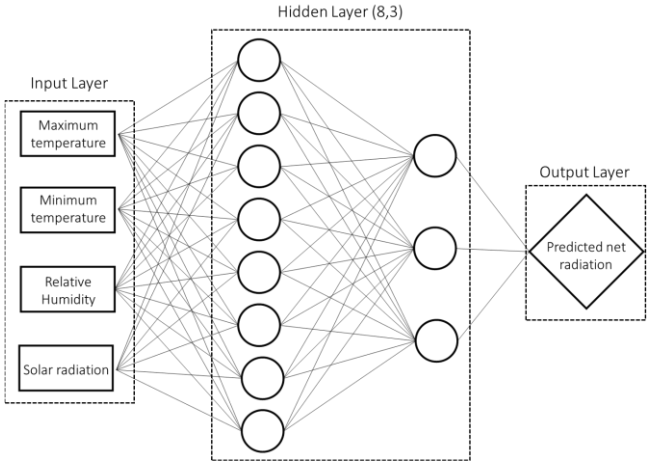

Fig. 5 The structure of ANN model in this study.

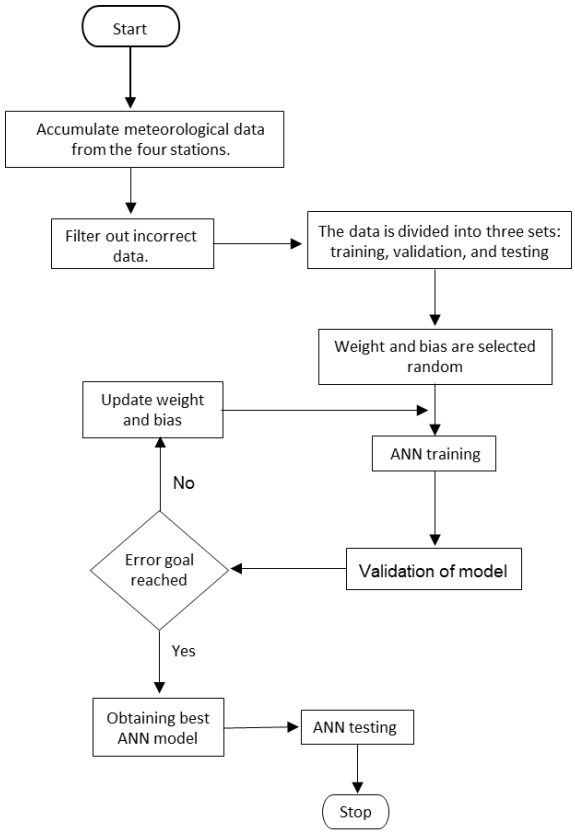

Fig. 6 The operation flowchart of the method.

After that, we choose the model validation measures and model, which are the coefficient of determination (R^2), the root mean square error relative to the mean measured values (RMSE), and the mean bias error relative to the mean measured values (MBE). We can be found from the scattering plot between the model result and measurement result and calculate the following equations (10-12).

$$R^2 = \frac{\left[\sum_{i=1}^{N} R_{n,model,i} \bullet R_{n,meas,i} - \frac{\left(\sum_{i=1}^{N} R_{n,model,i}\right)\left(\sum_{i=1}^{N} R_{n,meas,i}\right)}{N}\right]^2}{\left[\sum_{i=1}^{N} R_{n,model,i}^2 - \frac{\left(\sum_{i=1}^{N} R_{n,model,i}\right)^2}{N}\right]\left[\sum_{i=1}^{N} R_{n,meas,i}^2 - \frac{\left(\sum_{i=1}^{N} R_{n,meas,i}\right)^2}{N}\right]} \quad (10)$$

$$RMSE = \frac{\sqrt{\frac{\sum_{i=1}^{N}(R_{n,model,i} - R_{n,meas,i})^2}{N}}}{\frac{\sum_{i=1}^{N} R_{n,meas,i}}{N}} \times 100\% \quad (11)$$

$$MBE = \frac{\frac{\sum_{i=1}^{N}(R_{n,model,i} - R_{n,meas,i})}{N}}{\frac{\sum_{i=1}^{N} R_{n,meas,i}}{N}} \times 100\% \quad (12)$$

Where $R_{n,model,i}$ is net radiation from ANN model (MJ/m^2), $R_{n,meas,i}$ is net radiation from measurement (MJ/m^2), and N is total amount of data. The R^2 equal to one, and RMSE and MBE equal to zero indicated that the results of the model and the measurement are in good agreement.

3. Results and discussion

In this work, we estimate daily net radiation from meteorological data using the ANN model, and the results are shown in the scatter plot in Fig. 7 and time series plot in Fig. 8-11.

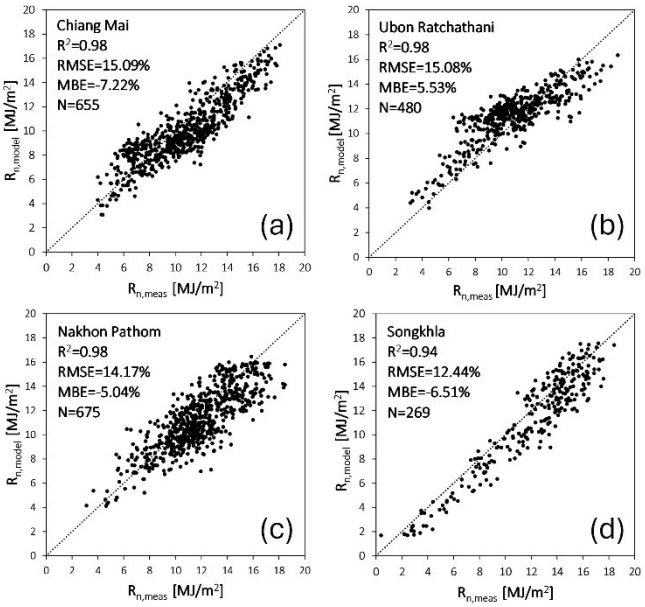

Fig. 7 The scatter plot of 4 stations compares the results of the model and the measurement. (a) Chiang Mai, (b) Ubon Ratchathani, (c) Nakhon Pathom, and (d) Songkhla.

Fig. 7 shows the comparison plots for various meteorological stations, showcasing the consistent validation of the model across locations. At Chiang Mai, the model achieved R^2 = 0.98, RMSE = 15.09%, and MBE = -7.22% (Fig. 7a). Ubon Ratchathani also displayed strong performance with R^2 = 0.98, RMSE = 15.08%, and MBE = 5.53%, (Fig. 7b). Similarly, Nakhon Pathom reported R^2 = 0.98, RMSE = 14.17%, and MBE = -5.04% (Fig. 7c). Lastly, Songkhla exhibited R^2 = 0.94, RMSE = 12.44% and MBE = -6.51% (Fig. 7d). Overall, all stations demonstrated robust model performance with high R^2 values (0.98) and low RMSE (14.48%). The performance of models of each station and combined data can be shown in Table 3.

Table 3. The summary of the statistical values of each station and combined data.

Stations	RMSE (%)	MBE (%)	R^2
CM	15.09	-7.22	0.98
UB	15.08	-5.53	0.98
NP	14.17	-5.04	0.98
SK	12.44	-6.51	0.94
Combined data	14.48	-2.17	0.98

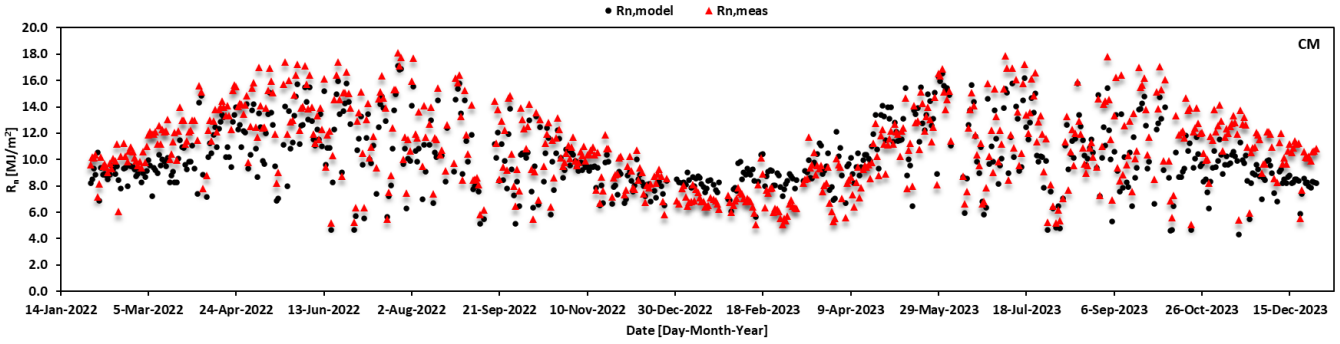

Fig. 8 The time series plot of the comparison between net radiation from model and net radiation from measurement at Chiang Mai.

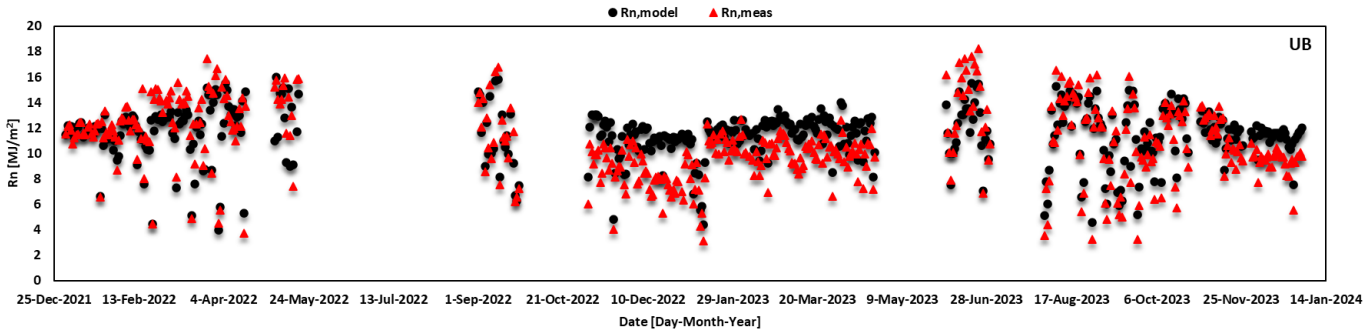

Fig. 9 The time series plot of the comparison between net radiation from model and net radiation from measurement at Ubon Ratchathani.

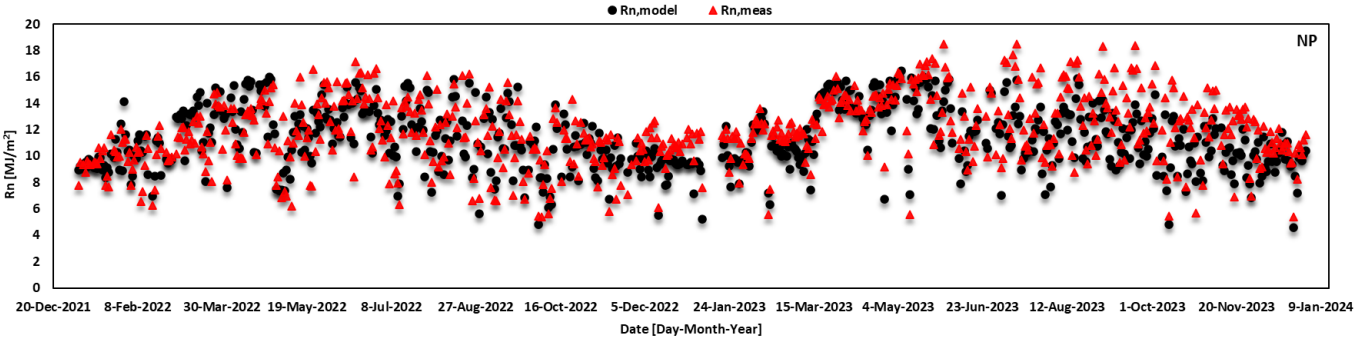

Fig. 10 The time series plot of the comparison between net radiation from model and net radiation from measurement at Nakhon Pathom.

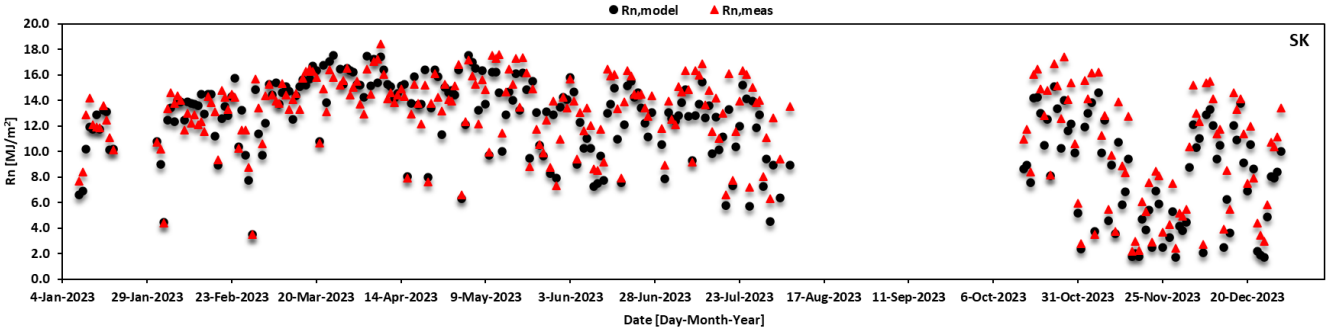

Fig. 11 The time series plot of the comparison between net radiation from model and net radiation from measurement at Songkhla.

Figure 8-11 presents a time series comparison of the model-predicted net radiation with actual measurements at four meteorological stations: CM, UB, NP, and SK. CM station, the model's slight underestimation of net radiation at CM is likely due to the measurement station's proximity to a road and a white fence, which can influence reflected shortwave radiation and emitted longwave radiation. UB station, the model's overestimation, particularly during winter, might be attributed to insufficient winter data for model training. This limited dataset could have led to inaccuracies in the model's winter predictions. NP station, the model's occasional underestimation at NP could be influenced by the higher surface humidity in the agricultural area of NP, which can impact energy balance processes. SK station, the consistent underestimation at SK is likely due to the highly variable weather conditions, with frequent transitions from sunny mornings to rainy evenings. This variability can challenge the model's ability to accurately capture the complex energy balance dynamics. The gaps in the data for UB and SK stations were caused by various net radiometer failures, including underground cable damage, battery depletion, and disturbances from animals, given the outdoor installation of the instruments.

Due to the varying structural constraints of ANN models across different research studies, we have compared the results obtained from this study with those of previous empirical models that utilized similar input variables (equations 3-5). The comparison results are presented in Table 4.

Table 4. Results of comparison between Proposed model (ANN) against other models.

Stations	Statistical values	Proposed model	Irmak et al. (Eq.3)	Alados et al. (Eq.4)	Tohsing et al. (Eq.5)
CM	RMSE	15.09	21.98	19.81	19.30
	MBE	-7.22	2.40	-4.57	-1.95
	R^2	0.98	0.95	0.96	0.96
UB	RMSE	15.08	24.50	19.67	19.70
	MBE	-5.53	-2.25	-4.42	-5.62
	R^2	0.988	0.94	0.97	0.96
NP	RMSE	14.17	21.82	20.18	18.19
	MBE	-5.04	-13.40	-13.38	-9.43
	R^2	0.98	0.97	0.98	0.97
SK	RMSE	12.44	15.57	16.66	12.32
	MBE	-6.51	-9.56	13.23	-7.37
	R^2	0.94	0.90	0.99	0.99

The four models showed strong agreement with the observed data. Solar radiation, a common input, was identified as a key variable in net radiation estimation. Tohsing et al. (Eq.5) and Alados et al. (Eq.4) models, which incorporated varying surface coefficients, outperformed the others in terms of accuracy and agreement with measured data, highlighting the importance of considering surface characteristics in such models. Statistical analysis indicates that the ANN model provides a better estimation of net radiation. This is attributed to the ANN's exceptional ability to analyze large datasets and complex relationships.

4. Conclusion

In this work, we estimate net radiation from meteorological data using an artificial neural network model. The location of the station is in the main region of Thailand, namely Chiang Mai meteorological station, Ubon Ratchathani meteorological station, Nakhon Pathom meteorological station, and Songkhla meteorological station, and we recorded data from 2017 to 2023 for training and testing the model. The results are satisfactory for the comparison, as shown in the time series plot and scatter plot between the model and the measurement. The time series plot comparison shows that their validation characteristics are very consistent. In the scatter plot, we use indicators of the performance model as shown in terms of R^2, RMSE and MBE which showed 0.98, 14.48% and -2.17%, respectively. Indicating the performance of the model is good, when compared to other studies, the developed model in this research produced superior results.

Acknowledgements

My appreciation also goes to the faculty and staff in the Department of Physics at Silpakorn University, Nakhon Pathom, whose resources and assistance have been invaluable. I would also like to acknowledge my peers for their camaraderie and the stimulating discussions that inspired me throughout my academic journey.

Finally, my sincere thanks to the Meteorological staff who provides research information support.

References

[1] Ojo, O. S., Emmanuel, I., Adeyemi, B. and Ogolo, E. O., Effect of the radiation balance on warming occurrence over west Africa. *Scientific African.* 11 (2021) 1-17, doi: https://doi.org/10.1016/j.sciaf.2021.e00700.

[2] Da Cunha, A. R., Schöffel, E. R. and Volpe, C. A., Estimation of evapotranspiration by various net radiation estimation formular for non-irrigated grass in Brazil. *Journal of Water Resource and Protection.* 6 (2014) 1-11, doi: https://doi.org/10.4236/jwarp.2014.615131.

[3] Lorenz, D. J., DeWeaver, E. T. and Vimont, D. J., Evaporation change and global warming: The role of net radiation and relative humidity. *Journal of Geophysical Research: Atmospheres*. 115 (2010) 1-13, doi: https://doi.org/10.1029/2010JD013949.

[4] Wang, K. and Liang, S., Estimation of daytime net radiation from shortwave radiation measurements and meteorological observations. *Journal of Applied Meteorology and Climatology*. 48 (2009) 634-643, doi: https://doi.org/10.1175/2008JAMC1959.1.

[5] Irmak, S., Irmak, A., Jones, J. W., Howell, T. A., Jacobs, J. M., Allen, R. G. and Hoogenboom, G., Predicting daily net radiation using minimum climatological data. *Journal of Irrigation and Drainage Engineering*. 129(4) (2003) 256-269, doi: https://doi.org/10.1061/(ASCE). 07339437(2003)129:4(256).

[6] Alados, I., Foyo-Moreno, I., Olmo, F. J. and Alados-Arboledas, L., Relationship between net radiation and solar radiation for semi-arid shrub-land. *Agricultural and Forest Meteorology*. 116(3-4) (2003) 221-227, doi: https://doi.org/10.1016/S0168-1923(03)00038-8.

[7] Carmona, F., Rivas, R. and Caselles, V., Development of a general model to estimate the instantaneous, daily, and daytime net radiation with satellite data on clear-sky days. *Remote Sensing of Environment.* 171 (2015) 1-13, doi: https://doi.org/10.1016/j.rse.2015.10.003.

[8] Limhoon, P. and Bualert, S., Variation of net radiation and solar spectrum in Thailand. *International Journal of Environmental Science and Development.* 4(2) (2013), doi: https://doi:10.7763/IJESD.2013.V4.315.

[9] Tohsing, K., Phoemwong, C., Uearsri, C. and Saiplang, P., An estimation of net radiation from global solar radiation in the main regions of Thailand. *Journal of Physics: Conference Series.* 2431 (2023) 1-4, doi: https:// doi.10.1088/1742-6596/2431/1/012021.

[10] Ferreira, A. G., Soria-Olivas, E., López, A. J. S. and Lopez-Baeza, E., Estimating net radiation at surface using artificial neural networks: a new approach. *Theoretical and applied climatology*. 106 (2011) 263-279, doi: https:// doi.10.1007/s00704-011-0488.

[11] Jiang, B., Zhang, Y., Liang, S., Zhang, X. and Xiao, Z., Surface daytime net radiation estimation using artificial neural networks. *Remote Sensing*, 6(11) (2014) 11031-11050, doi: https:// doi:10.3390/rs61111031.

[12] Aweda, F. O. and Adebayo, S., Estimation of net radiative measurement of meteorological parameters at Iwo, Nigeria in 2018. *Zimbabwe Journal of Science and Technology,* 15 (2020) 23-33.

[13] Ozturk, M., Salman, O. and Koc, M., Artificial neural network model for estimating the soil temperature. *Canadian Journal of Soil Science.* 91(4) (2011) 551-562, doi: https://doi.org/10.4141/cjss10073.

[14] Patel, D., Patel, S., Patel, P. and Shah, M., Solar radiation and solar energy estimation using ANN and Fuzzy logic concept: A comprehensive and systematic study. *Environmental Science and Pollution Research.* 29 (2022) 32428-32442, doi: https://doi:10.1007/s11356-022-19185-z.

[15] Bishop, C. M. *Neural Networks for Pattern Recognition*. Oxford University Press, 1995.

[16] Khanna, T. *Foundations of Neural Networks*. Addison-Addison-Wesley, 1990.

[17] Haykin, S. *Neural Networks and Learning Machines*. 3rd edn., Pearson Education India, 2009.

[18] Goodfellow, I., Bengio, Y., and Courville, A. *Deep Learning*. MIT Press, 2016.